Supporting Information for

Intraseasonal shift in the wintertime North Atlantic jet structure projected by CMIP6 models

Marina García-Burgos[1,2], Blanca Ayarzagüena[1], David Barriopedro[2], Tim Woollings[3] and Ricardo García-Herrera[1,2]

[1] *Departamento de Física de la Tierra y Astrofísica, Universidad Complutense de Madrid, 28040 Madrid, Spain.*

[2] *Instituto de Geociencias (IGEO), CSIC-UCM, 28040, Madrid, Spain.*

[3] *Department of Physics, Atmospheric, Oceanic and Planetary Physics, University of Oxford, Parks Rd, Oxford OX1 3PU, UK*

Contents of this file

Figs. S1 to S3 and Table S1

Introduction

Supplementary material TableS1 and Figs. S1 to S3 are included:

- Fig. S1 is the multi-model mean change in the 850hPa zonal wind during the extended winter (NDJF)
- Fig. S2 is the distributions of the simulated EDJ Lat by GCMs
- Fig. S3 is the historical (1979-2009) distribution of the latitude of the North Atlantic eddy-driven jet for biased and neutral global climate models.
- Table S1 contains a list of the model and ensemble members used in this study.

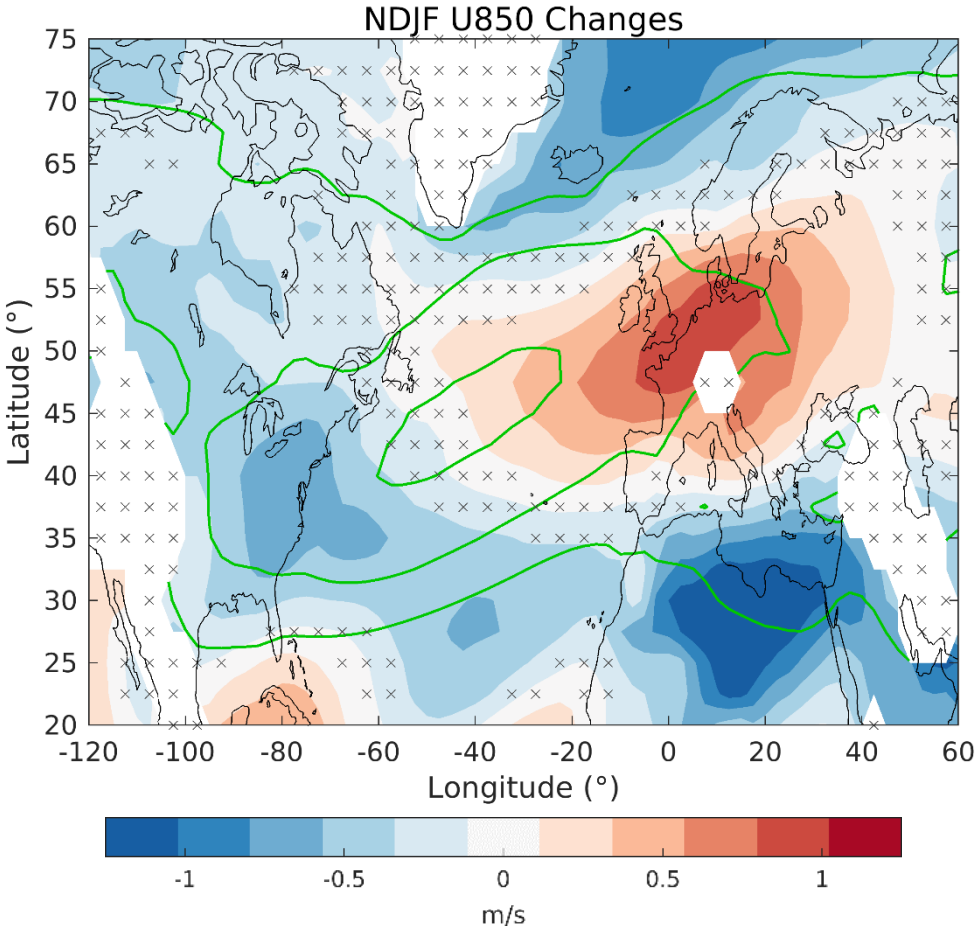

Fig. S1: Winter projections of the EDJ: Multi-model mean of the climate change signal in the winter (NDJF) zonal wind at 850hPa (shading, [m/s]). The 1979-2009 NDJF climatology is shown with contours (starting at 2m/s and drawn every 4m/s). Crosses indicate the grid-points with no significant differences at the 95% confidence level (after a 1,000-trial Monte Carlo test) and masked grid-points. The mask is constructed as the set of grid-points where the GCMs do not present data at 850hPa.

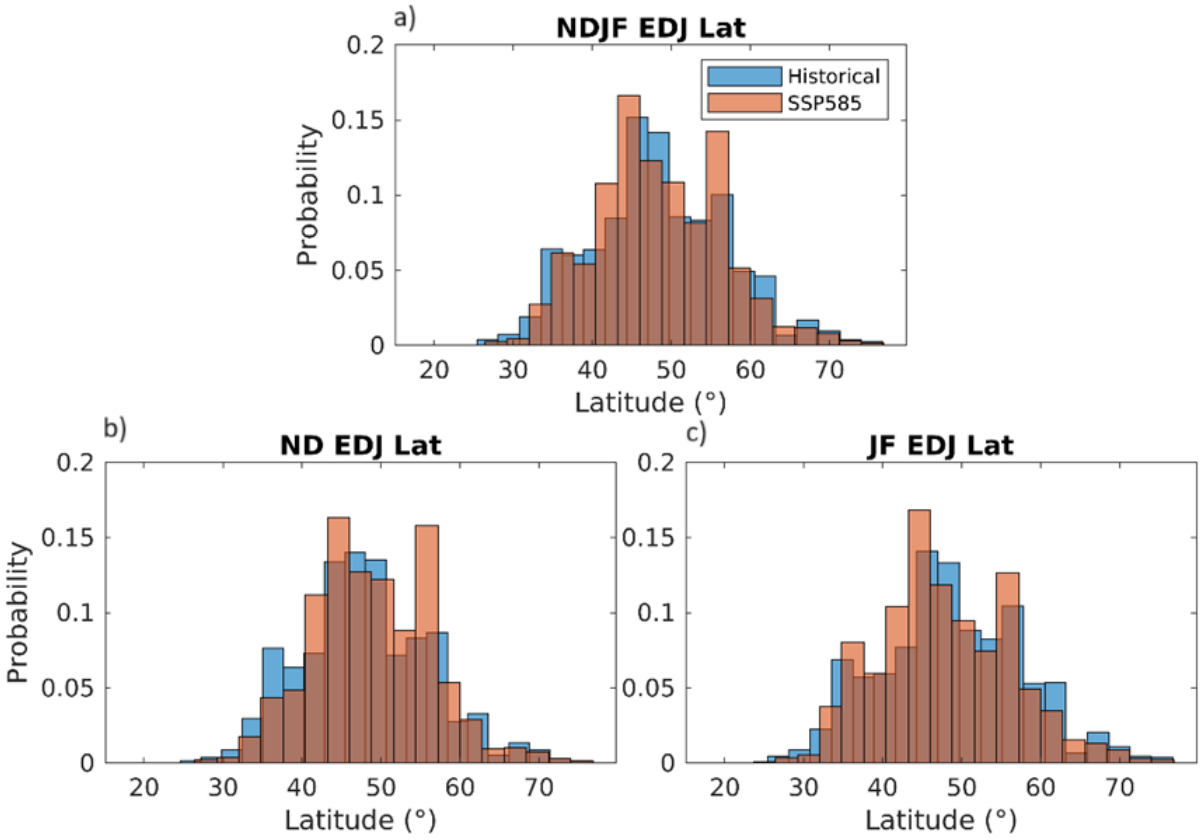

Fig. S2: Distributions of the EDJ Lat simulated by the GCMs in Historical (blue) and SSP5.85 (red) experiments, for the whole (a), early (b) and late (c) winter.

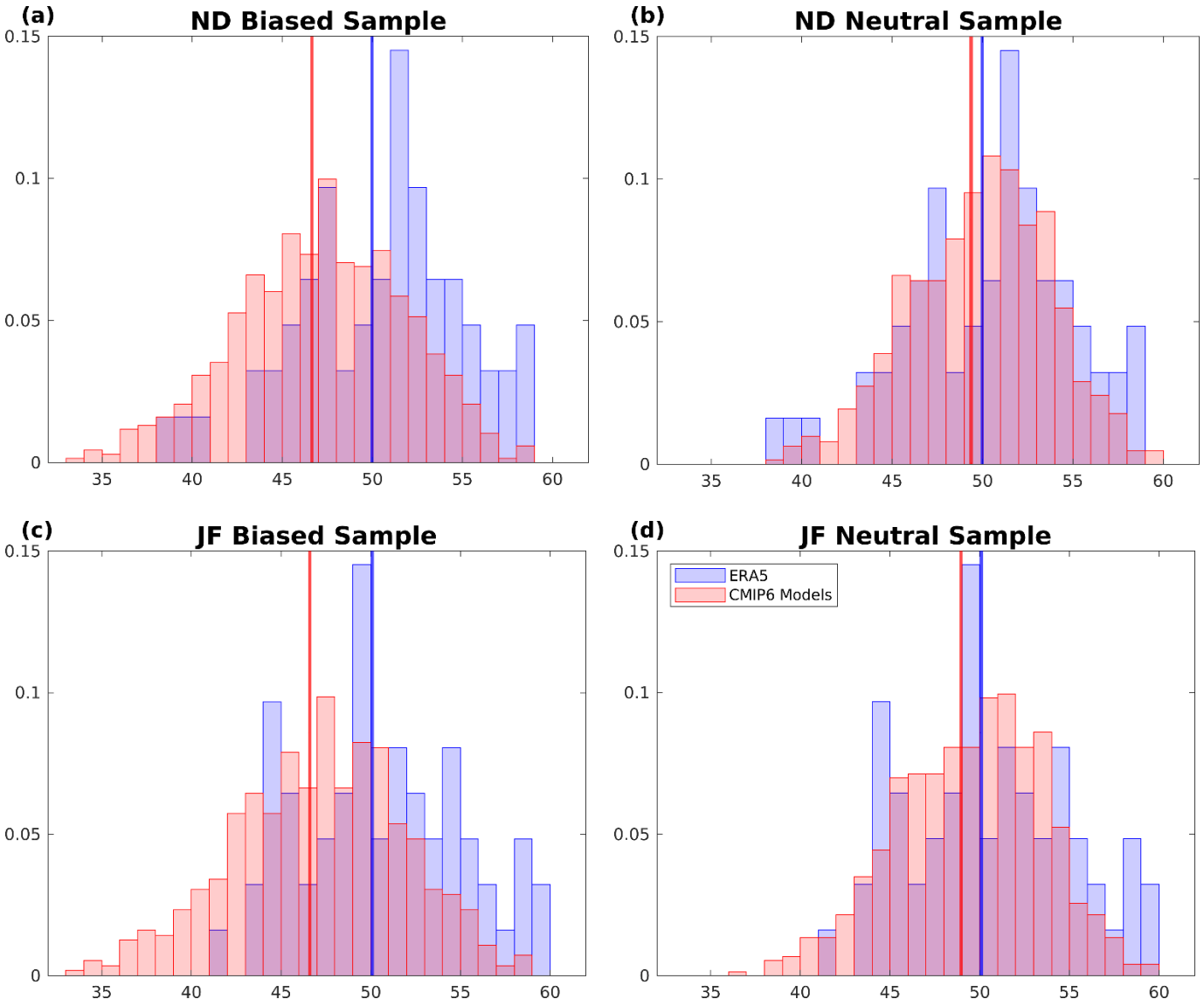

Fig. S3: Distributions of the monthly latitude of the North Atlantic eddy-driven jet during the early (**a, b**) and late (**c, d**) winters of the period 1979-2009 for ERA5 (purple) and: (**a, c**) biased, and; (**b, d**) unbiased models of the CMIP6 (pink) (see Methods in the main text). For each panel, all models are pooled together, and the frequency distributions are normalized to add 1.

Table S1: List of global climate models included in the study, the considered ensemble member (rXiXpXfX: where r corresponds to Realization, i to Initialization, p to Physics, and f to Forcing) and the resolution specifications.

Global Climate Model	Ensemble Member	Atmospheric Resolution Model
BCC-CSM2-MR	r1i1p1f1_gn	1.125° x 1.125 L46, top 1.46 hPa
CAMS-CSM1-0	r2i1p1f1_gn	1.125° x 1.125 L31, 10 hPa
CanESM5	r1i1p2f1_gn	T63L49, top 1 hPa
CESM2	r1i1p1f1_gn	1° × 1° L32, top 40 km
CESM2-WACCM	r1i1p1f1_gn	1° × 1° L70, top 150km
CMCC-CM2-SR5	r1i1p1f1_gn	1.25° x 0.9° L30, top ~2 hPa
CMCC -ESM2	r1i1p1f1_gn	1.25° x 0.9° L30, top ~2 hPa
CNRM-CM6-1	r1i1p1f2_gr	T127 91L, top 78.4 km
CNRM-ESM2-1	r1i1p1f2_gr	T127 91L, top 78.4 km
EC-Earth3	r1i1p1f1_gr	TL255 L91, top 0.01 hPa
EC-Earth3-Veg	r1i1p1f1_gr	TL255 L91, top 0.01 hPa
FGOALS-g3	r1i1p1f1_gn	2° x 2° L26, top 2.19 hPa
HadGEM3-GC31-LL	r1i1p1f3_gn	N96 L85, top 85 km
INM-CM4-8	r1i1p1f1_gr1	2° x 1.5° L21, top 0.01 sigma
INM-CM5-0	r1i1p1f1_gr1	2° x 1.5° L73, top 0.2 hPa
IPSL-CM6A-LR	r1i1p1f1_gr	N96 L79, top 80 km
MIROC6	r1i1p1f1_gn	T85 L81, top 0.004 hPa
MIROC-ES2L	r1i1p1f2_gn	T42 L40; top 3 hPa
MPI-ESM1-2-HR	r1i1p1f1_gn	T127 L95, top 0.01 hPa
TaiESM1	r1i1p1f1_gn	1.25° x 0.9° L30, top ~2 hPa
UKESM1-0-LL	r1i1p1f2_gn	N96 L85, top 85 km